Appl Nanosci (2014) 4:927–934
DOI 10.1007/s13204-013-0270-5

ORIGINAL ARTICLE

Amperometric biosensor of SnO_2 thin film modified by Pd, In and Ag nanostructure synthesized by CSP method

Marwa Abdul Muhsien Hassan · Areej Adnan Hateef · Aseel Mustafa Abdul Majeed · Ali Jasim Mohammed Al-Jabiry · Sabah Jameel · Haidar Abdul Razaq Abdul Hussian

Received: 20 June 2013 / Accepted: 4 September 2013 / Published online: 24 October 2013

Abstract Palladium, Indium and Silver-doped SnO_2 thin film was deposited by chemical spray pyrolysis on ITO and porous silicon substrates to be a fast $MgSO_4{\cdot}7H_2O$ amperometric biosensor. The prepared SnO_2 films were doped by dipping in palladium chloride $PdCl_2$, indium chloride, $InCl_3$ and silver nitrides $AgNO_3$ dissolved in ethanol C_2H_5OH. The structural and optical properties of the prepared films were studied. The sensitivity behaviors of SnO_2, SnO_2: Pd, SnO_2: In and SnO_2: Ag based on the amperometric biosensor to $MgSO_4{\cdot}7H_2O$ salts were investigated at room temperature with different doping.

Keywords SnO_2 · Spray pyrolysis · Optical properties · Biosensor · AFM · (Palladium, Indium and Silver) catalyst · Porous silicon · ITO

Introduction

Tin oxide (SnO_2), a wide band gap semiconductor, is well-known for its excellent gas sensitivity (Du et al. 2009; Chen et al. 2005) and its use in fabricating transparent conductive glasses (Shen et al. 2009). SnO_2 nanostructures have also been investigated for photoluminescence (Chen et al. 2009), lasing (Cheng et al. 2009), field emission (Zhang et al. 2009), transistors, solar cells (Tennakone et al. 1999) and lithium ion batteries (Du et al. 2009; Liu et al. 2009). In particular, SnO_2 is biocompatible (Jia et al. 2005; Ansari et al. 2009; Feng et al. 2009), cheaper than Si, more stable than ZnO in physiological environment and more conductive than TiO_2 (Kafi et al. 2008). Despite these, there is no report yet on applying SnO_2 nanostructure biosensors.

The aim of this work is to elucidate the sensing mechanism of the SnO_2, SnO_2: Pd, SnO_2: In and SnO_2: Ag biosensor by using spray pyrolysis techniques.

Experimental work

The chemical techniques for the preparation of thin films have been studied extensively because such processes facilitate the designing of materials on a molecular level. The chemical spray pyrolysis is one of the chemical techniques applied to form a variety of thin films, resulting in good productivity from an uncomplicated apparatus. A 0.1 M concentration aqueous precursor solution of tin chloride ($SnCl_4{\cdot}5H_2O$) has been prepared by dissolving a solute quantity of 3.5085 g of $SnCl_4{\cdot}5H_2O$ in 100 mL dissolved in ethanol alcohol C_2H_5OH and distilled water has been employed in getting SnO_2 thin films. A magnetic stirrer is incorporated for this purpose for about 10–15 min. Prior to depositing the films, the ITO glass substrates were thoroughly cleaned in distilled water and dried in air for 5 min. After that, they were soaked in alcohol to remove any stains and contaminants. The substrate temperature was maintained within 450 ± 5 °C during the deposition period. The film thickness was controlled by both the precursor concentration and the number of sprays, or alternatively, spraying time. Thus, a 5 s spraying time is maintained during the experiment with specific nitrogen carrier gas pressure. The spray rate of solution was maintained at 3.5 mL min^{-1} throughout the experiment.

M. A. M. Hassan (✉) · A. A. Hateef · A. M. A. Majeed · A. J. M. Al-Jabiry · S. Jameel · H. A. R. A. Hussian
Physics Department, College of Science, Al-Mustansiryah University, Baghdad, Iraq
e-mail: marwa_alganaby@yahoo.com

Table 1 Optimum thermal spray pyrolysis deposition conditions for the preparation of SnO_2 thin films

Spray parameters	Values
Concentration of precursor	0.1 M
Volume of precursor sprayed	100 mL
Solvent	Ethanol alcohol and distilled water
Substrate temperature	450 ± 5 °C
Spray rate	3.5 mL/min
Nozzle-substrate distance	25 cm

Table 1 summarizes the optimized thermal pyrolysis deposition conditions for the preparation of SnO_2 thin films that were employed in the current research.

The possible chemical reaction that takes place on the heated substrate to produce SnO_2 thin film may be described by the following reaction as shown in Fig. 1:

$$SnCl_4\ (ad) + 2H_2O\ (g) \overset{heat}{\rightarrow} SnO_2\ (ad) + 4HCl\ (g) \qquad (1)$$

Schematic diagram of doped SnO_2 films' structure, inclusive of fine-dispersed phases, is shown in Fig. 2.

In the current research, tin oxide thin films were deposited on ITO glass and porous silicon substrates employing spray pyrolysis deposition chamber whose main components set up is illustrated in the schematic diagram of Fig. 3. It is essentially made up of a precursor solution, carrier gas assembly connected to a spray nozzle, and a temperature-controlled hot plate heater.

The precipitated SnO_2 on the ITO glass substrate was in the form of nanocrystals which is clearly identified by the AFM morphology studies of SnO_2 nano-films. Metal oxide biosensors need a catalyst deposited on the surface of the film to accelerate the reaction, increase the sensitivity, and to improve the response time of the detector (Abhijith 2006). Small amounts of noble metal additives, such as Pd

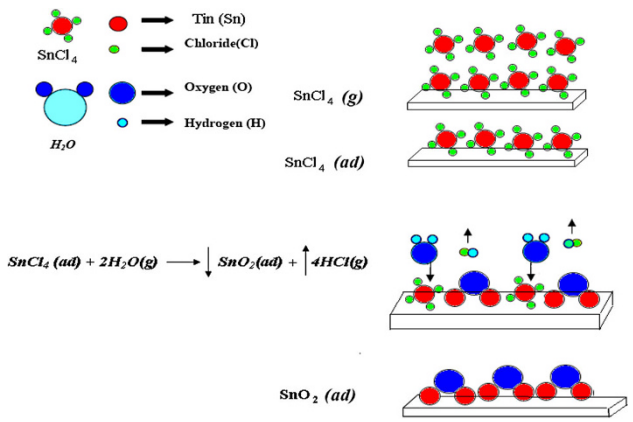

Fig. 1 The chemical reaction of the SnO_2 growth on the substrate

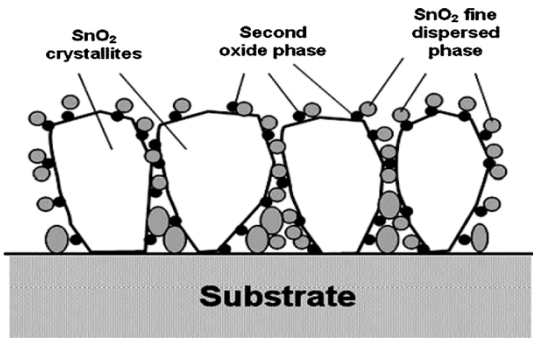

Fig. 2 Schematic diagram of the structure of SnO_2-doped films

or Pt or Ag are commonly dispersed on the semiconductor as activators or sensitizers to improve the gas selectivity, sensitivity and to lower the operating temperature as pointed out (Patrícia et al. 2001). For the above reasons, the surface of the deposited SnO_2 thin films was catalyzed using successive multiple dipping of the prepared samples in a 50 cm^3 solution made up of dissolving 5 % by weight palladium chloride $PdCl_2$, indium chloride, $InCl_3$ and silver nitrides $AgNO_3$ in ethyl alcohol C_2H_5OH. Each sample was successively dipped 25 times for about 3–5 s. After each dipping, the sample was heated to 50 °C in evacuated oven for 3 min to facilitate the evaporation of the volatile ethyl alcohol. Finally, the dipped samples were heat-treated at 300 °C for 1 h in an evacuated oven. An eight-finger metal mask was used to thermally evaporate the aluminum interdigitated electrodes on the doped SnO_2 samples. Both the spacing between the mask fingers and their width were equal to 1 mm. This design has proven to be reliable throughout our work. The porous silicon substrate was fabricated from a p-type (100) silicon wafer of low resistivity (0.01–0.02 Ω cm).The wafer was anodized in an electrochemical etching solution consisting of 24 %HF/ethanol/H_2O (Luongo et al. 2005). The wafer and platinum cathode were placed in a Teflon jig, schematically illustrated in Fig. 4. The surfaces of Si substrate and Pt cathode were kept parallel to each other and the current flow in the etchant was normal to the wafer surface. The wafer was etched at a current density of 50 mA/cm^2 for a 5 min. The wafer was then removed from the etching bath, rinsed with water, and cleaned. This resulted in formation of an array of nonporous normal to the wafer, all being parallel to each other.

Amperometric biosensor to 1 mg/L $MgSO_4{\cdot}7H_2O$ salts concentrations were investigated at room temperature with different doping (SnO_2, SnO_2: Pd, SnO_2: In and SnO_2: Ag), as one of the most popular biosensors, has been intensively investigated. Application of SnO_2 nanostructure in the $MgSO_4{\cdot}7H_2O$ biosensors just appeared in the last several years.

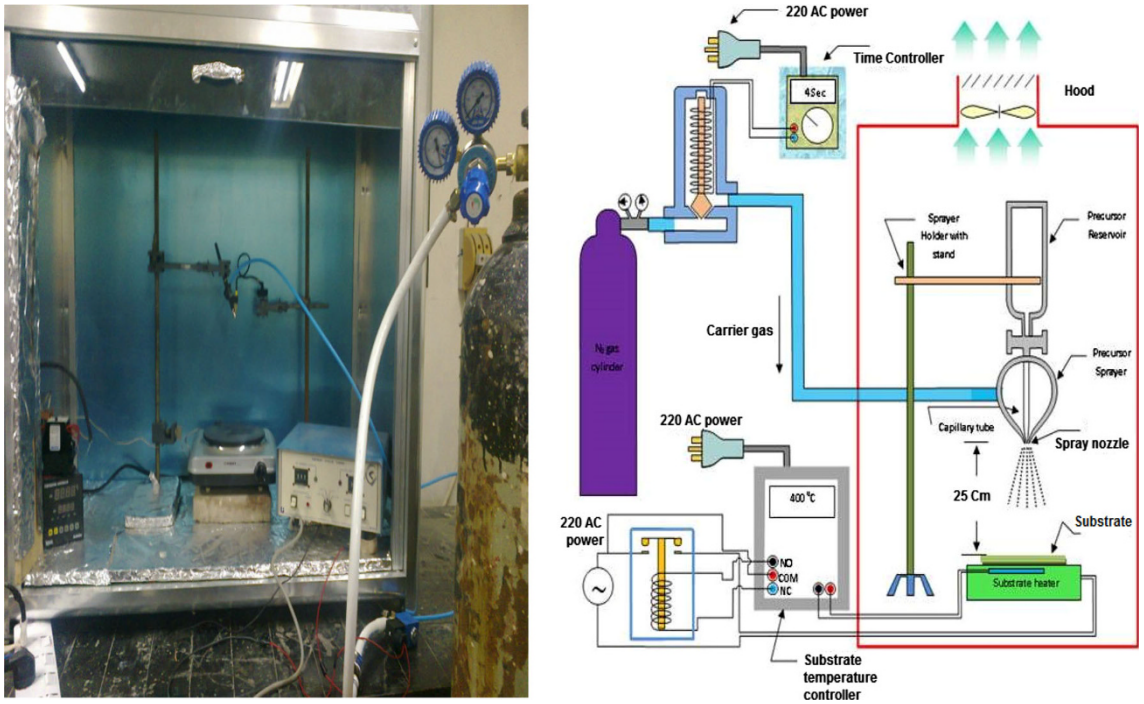

Fig. 3 Experimental set up of the spray pyrolysis deposition technique

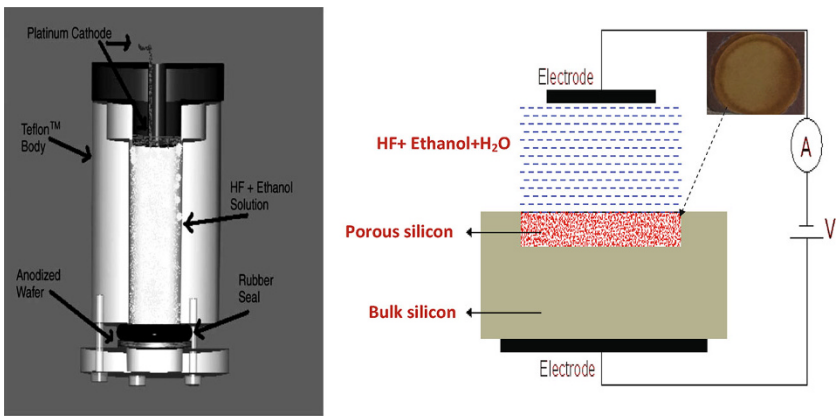

Fig. 4 Schematic illustration of the porous silicon etching setup

Results and discussion

The structure and lattice parameters of SnO_2 films were analyzed by a LabX XRD 6000 SHIMADZU XR-Diffractometer with Cu Kα radiation of (voltage 30 kV, current 15 mA, scanning speed = 4°/min), as illustrated in Fig. 5a and the effect of the Pd, In and Ag dopant on the structure of the film can be shown in Fig. 5b–d. Diffraction pattern was obtained with 2θ starting from 20° to 60° at 5° glancing angle. In both the as—deposited and Pd, In, Ag—doped SnO_2 thin films, the X-ray diffraction spectra possess one sharp and two small peaks. It means that the film is polycrystalline in nature and a tetragonal rutile structure with crystal planes (110), (101) and (211). The result is in a good agreement with data mentioned in the literature (JCPDF card no 03-0439, 02-1340 and 02-1337 Cassiterite, Tin Oxide). The strongest peak observed at $2\theta = 26.8665°$ ($d = 0.331579$ nm) can be attributed to the (110) plane of the tetragonal SnO_2. The (101) and (211) peaks were also observed at $2\theta = 34.0513°$ and 52.0273°, respectively, but two peaks are of much lower intensity than the (110) peak. The c-axis lattice constant of the SnO_2 thin film was calculated from XRD data as 0.315679 nm (Stanimirova et al. 2005; Boshta et al. 2010).

The optical transmittance spectra of the deposited film were recorded. The variation of optical transmittance ($\%T$) with wavelength λ of 0.1 M of the spray deposited tin oxide film at substrate temperature 450 °C. It was found that the average transmittance of the film is 81 % Fig. 6.

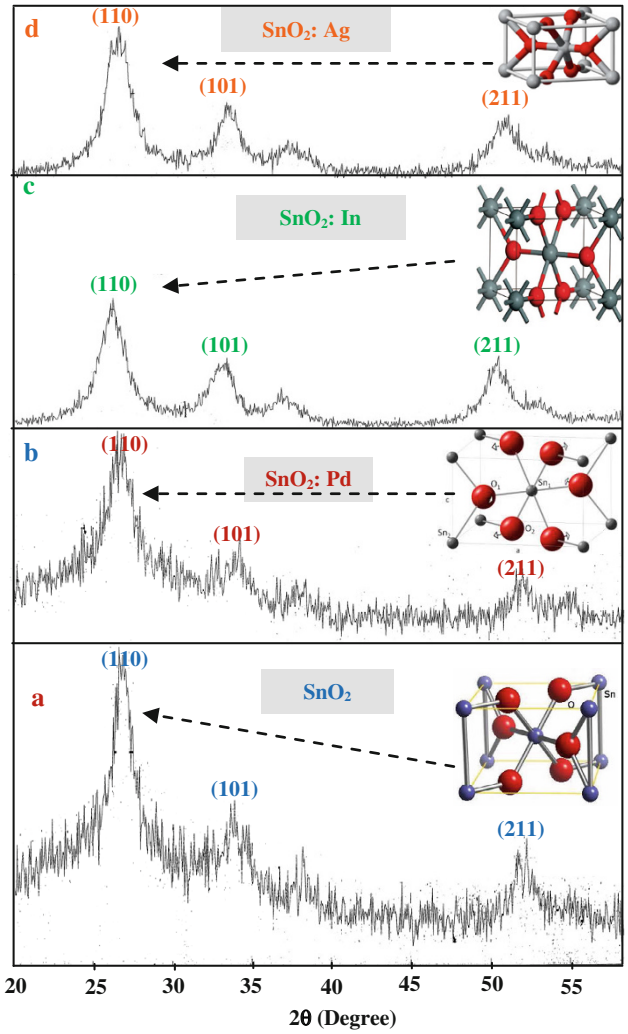

Fig. 5 XRD of as-deposited (**a**) SnO_2, (**b**) SnO_2: Pd, (**c**) SnO_2: In and (**d**) SnO_2: Ag thin film on ITO glass substrate at 450 °C

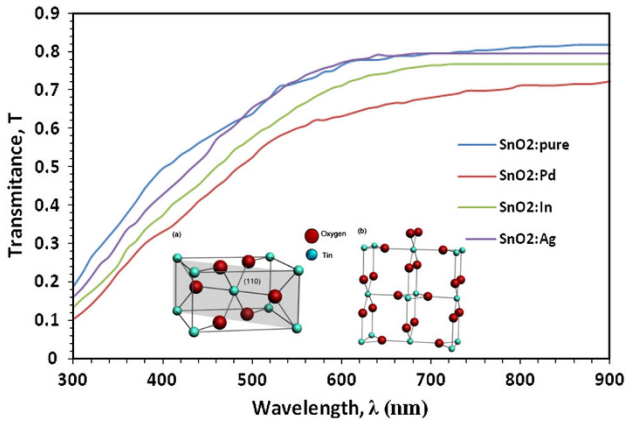

Fig. 6 Transmission spectrum of SnO_2, SnO_2: Pd, SnO_2: In and SnO_2: Ag thin films deposited on ITO glass substrate

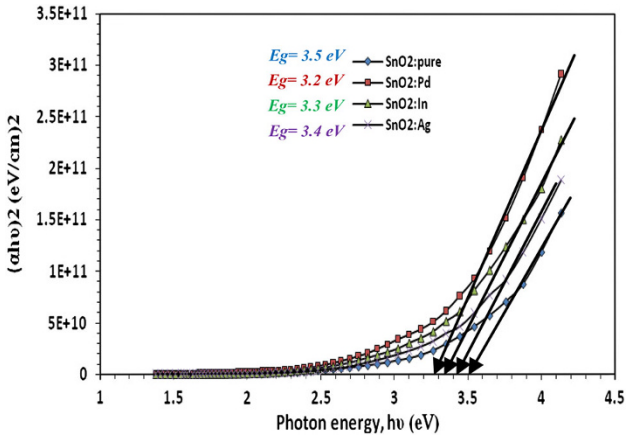

Fig. 7 Toue Plot of $(\alpha h\upsilon)^2$ with photon energy of SnO_2, SnO_2: Pd, SnO_2: In and :Ag thin films deposited on ITO glass substrate

The absorption coefficient can be calculated from the Lambert's formula (Mishra et al. 2009).

$$\alpha = (1/t)\log(1/T) \tag{2}$$

where, t is a thickness of the film, T is a transmittance of the film

Figure 7 shows the variations of $(\alpha hv)^2$ and (hv) for the determining the band gap E_g of SnO_2 film by extrapolation of curve. The incident photon energy is related to the direct band gap E_g by equation:

$$(\alpha hv) \infty \left(hv - E_g\right)^{1/2} \tag{3}$$

The optical band gap was estimated in lower wave length region and it was found to be 3.5 eV.

The morphology of SnO_2 and SnO_2: Pd, SnO_2: In and SnO_2: Ag sensing film surface was imaged by atomic force microscope (AFM) model AA3000 SPM from Angstrom Advanced Inc. Figure 8 shows the formation of SnO_2 nanostructure. The root mean square of the surface roughness prepared by this method is shown in Table 2. Figure 8 reveals the (2-D) and (3-D) AFM images of undoped and doped SnO_2 films. AFM micrographs prove that the grains are uniformly distributed within the scanning area (10,000 × 10,000 nm) with individual columnar grains extending upwards.

It was found that using (ethyl alcohol) (C_2H_5OH) organic solvent other than water is preferred. This is due to a better droplet size distribution and, also due to additional heat transfer toward the sample surface resulted from alcohol burning (Arca and Fleischer 2009).

Figure 9 shows the SEM micrographs of doped and undoped SnO_2/p-PSi/c-Si sensing film surface were carried out by (Hitachi FE-SEM model S-4160, Japan) in University of Tehran at 15 kV of SnO_2 films.

It is observed that the particles of different shapes and sizes are formed due to insufficient substrate temperature and doping for its homogenation. When the SnO_2 doping 5 %, silver larger crystallites are broken down to a smaller one. This causes relatively better homogeneity. The finely

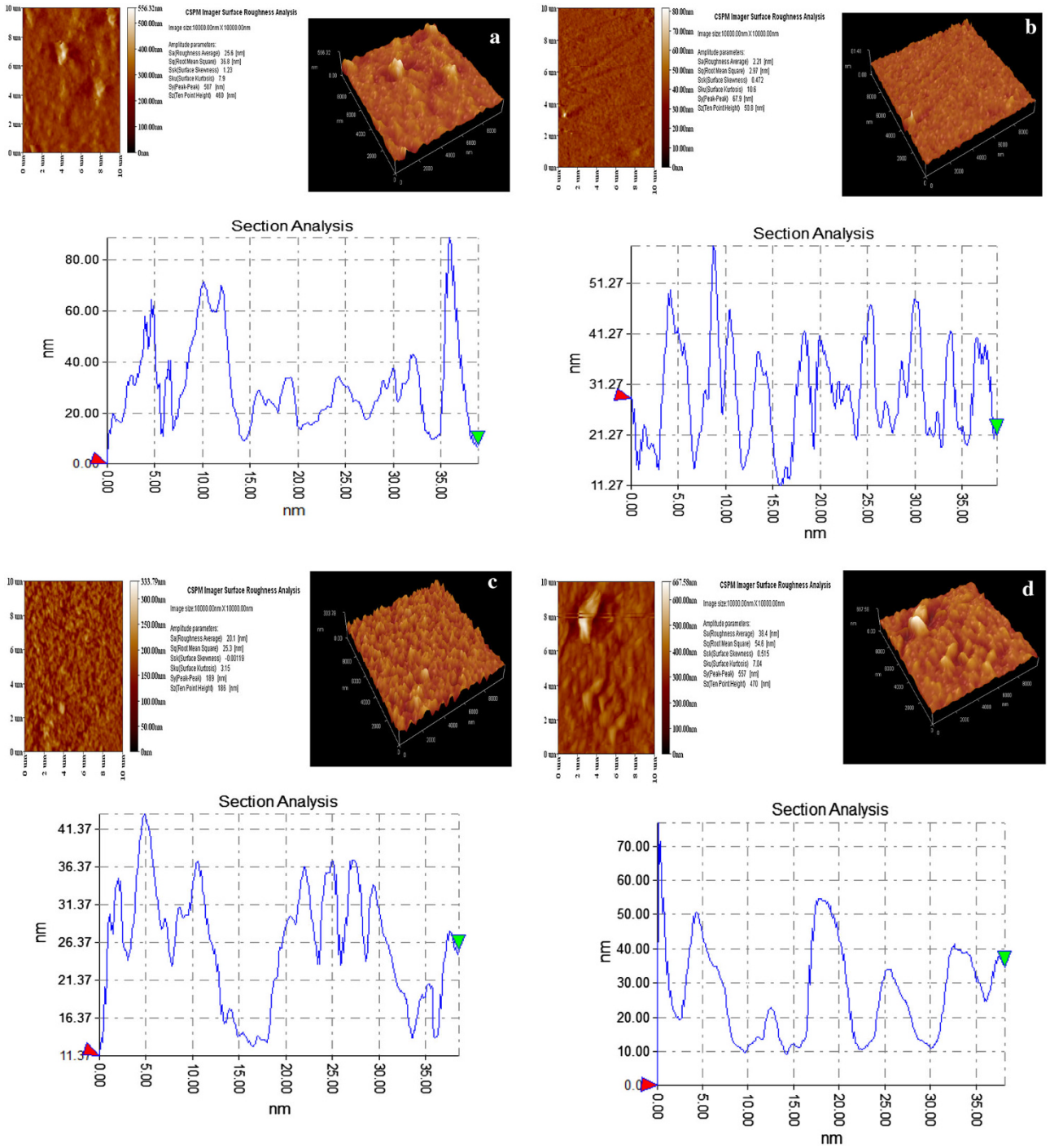

Fig. 8 AFM image of (**a**) SnO_2, (**b**) SnO_2: Pd, (**c**) SnO_2: In and (**d**) SnO_2: Ag thin film on ITO glass substrate at 450 °C

divided nanocrystalline monodispersed nanoparticles of SnO_2 are observed at doing 5 % palladium.

The biosensor sensitivity of a film is usually measured as the percentage change in film resistance on salt exposure, or may be defined as the ratio of its resistance in air to its steady state value in the presence of a salt, or vice versa. Irrespective of the definition one uses, it is important to monitor the (change in) electrical resistance of a sensor film. For measurement of change in resistance on exposure to salts, the sensor head was put in an air-tight chamber of volume 250 mL, a pre-defined concentration of salt taken from calibrated cannister of 1 mg/L $MgSO_4{\cdot}7H_2O$ solution was introduced in this chamber by syringe (Fig. 10).

Table 2 The results from AFM measurements of SnO_2 film prepared at different doping

Sample	S_a (roughness average) (nm)	S_q (root mean square) (nm)	S_z (ten-point height) (nm)
SnO_2	25.6	36.8	460
SnO_2: Pd	2.21	2.97	50.8
SnO_2: In	20.1	25.3	186
SnO_2: Ag	38.4	54.6	470

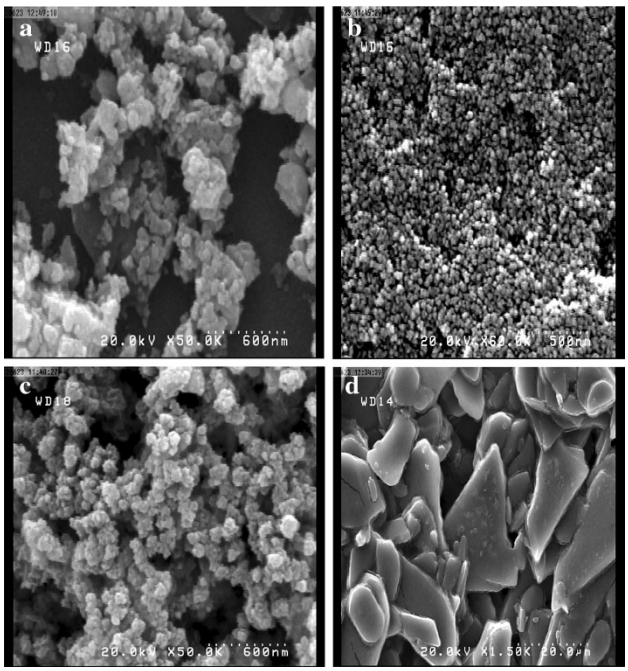

Fig. 9 SEM image of **a** SnO_2, **b** SnO_2: Pd, **c** SnO_2: In and **d** SnO_2: Ag thin film on porous silicon substrate at 450 °C

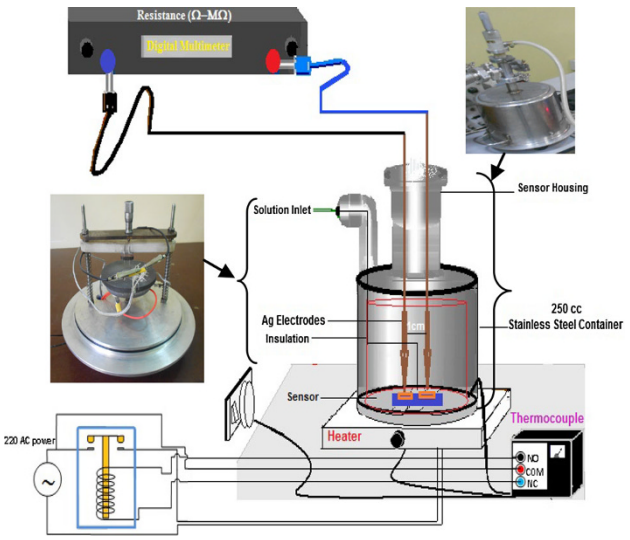

Fig. 10 Gas sensor unit

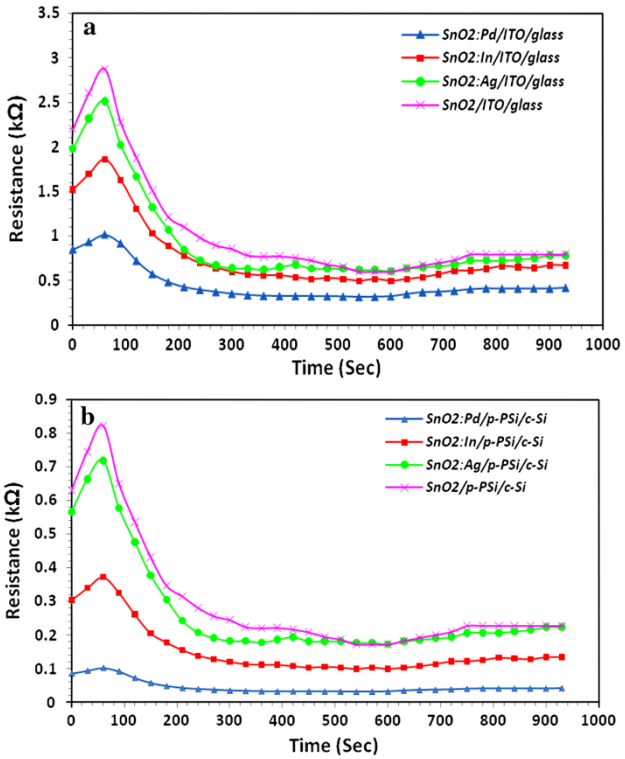

Fig. 11 Relation between resistance and time of SnO_2 film with different doping prepared on (**a**) ITO substrate and (**b**) p-PSi substrate

The resistance of the film was measured before and after exposure to salt.

$$\text{sensitivity}\ (\%) = |(R_{\text{salt}} - R_{\text{air}})/R_{\text{air}}| \times 100 \quad (4)$$

where R_a is the resistance in air and R_s is the resistance in a sample salt. Chemical interaction between the drop of 1 mg/L $MgSO_4{\cdot}7H_2O$ solution and tin oxide film caused some of the variations in the output signal recorded as resistance decrease of tin oxide film for all doping at room temperature, as shown in Fig. 11.

Figure 12 shows the sensitivity of doped and undoped SnO_2 films to 1 mg/L of $MgSO_4{\cdot}7H_2O$ solution salt as a function of working temperature. As evident, the sensitivity increases with the temperature and reaches a maximum value in correspondence of $T = 200$–300 °C. If the temperature increases again, the sensitivity decreases.

The sensitivity values of doped and undoped SnO_2 sensor film are plotted as a function of 1 mg/L $MgSO_4{\cdot}7H_2O$ solution salt concentration in Fig. 13. It is observed that the sensitivity slows down at higher concentration; this may be due to less availability of surface area with possible reaction sites on surface of the film.

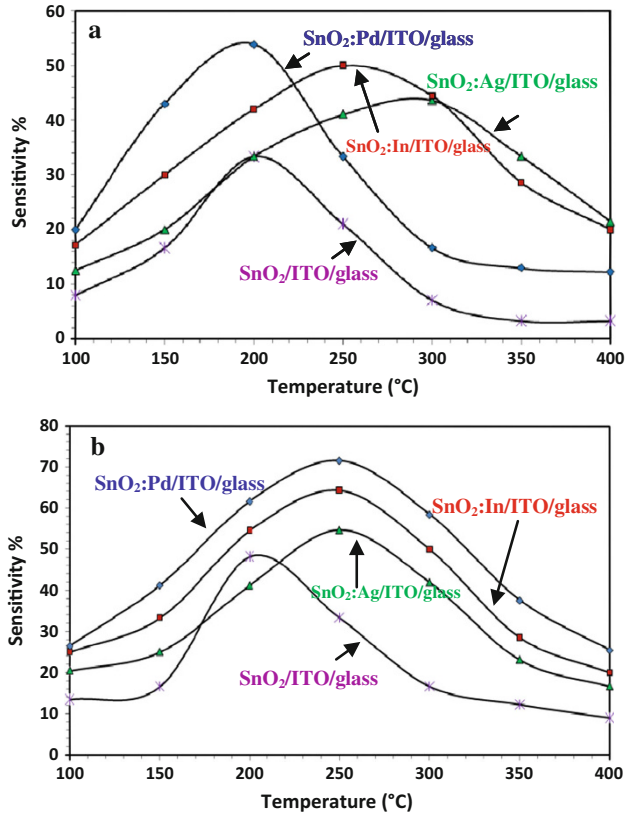

Fig. 12 Relation between sensitivity and temperature of SnO_2 film with different doping prepared on (**a**) ITO substrate and (**b**) p-PSi substrate

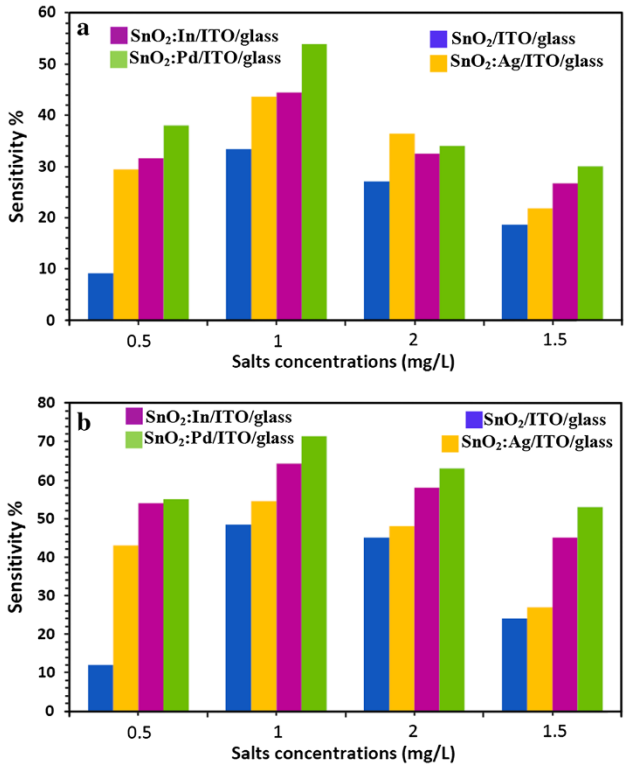

Fig. 13 Relation between sensitivity and salts concentration of SnO_2 film with different doping prepared on (**a**) ITO substrate and (**b**) p-PSi substrate

Conclusions

In this paper, we have reported on the preparation of palladium, indium and silver–doped SnO_2 thin film was deposited by chemical spray pyrolysis on ITO and porous silicon substrates to be a fast $MgSO_4{\cdot}7H_2O$ amperometric biosensor and on subsequent microstructural and physical characterizations. High-resolution scan electron microscopy observation evidenced compositional and structural modification. The XRD results reveal that the deposited thin film of doped and undoped SnO_2 has a good nanocrystalline rutile tetragonal phase structure. The AFM and SEM results demonstrate that a uniform surface morphology and the nanoparticles are fine with an average grain size of about 40–50 nm. Optical studies showed that the doped and undoped SnO_2 has high absorption coefficient ($\approx 104\ cm^{-1}$) with a direct band gap. The prepared SnO_2 films were doped by dipping in palladium chloride $PdCl_2$, indium chloride, $InCl_3$ and silver nitrides $AgNO_3$ dissolved in ethanol C_2H_5OH. The sensitivity behaviors of SnO_2, SnO_2: Pd, SnO_2: In and SnO_2: Ag based on the amperometric biosensor to $MgSO_4{\cdot}7H_2O$ salts were investigated at room temperature with different doping.

References

Abhijith N (2006) Semiconducting metal oxide gas sensors: development and related instrumentation. M.Sc. Thesis, Indian Institute of Science

Ansari AA, Kaushik A, Solanki PR, Malhotra BD (2009) Electrochemical cholesterol sensor based on tin oxide-chitosan nanobiocomposite film. Electroanalysis 21:965

Arca E, Fleischer K (2009) Influence of the precursors and chemical composition of the solution on the properties of SnO_2 thin films grown by spray pyrolysis. J Phys Chem C113:21074–21081

Boshta M, Mahmoud FA, Sayed MH (2010) Characterization of sprayed SnO_2: Pd thin films for gas sensing applications. J Ovonic Res 6(2):93–98

Chen YJ, Xue XY, Wang YG, Wang TH (2005) Synthesis and ethanol sensing characteristics of single crystalline SnO_2 nanorods. Appl Phys Lett 87:233503

Chen R, Xing GZ, Gao J, Zhang Z, Wu T, Sun HD (2009) Characteristics of ultraviolet photoluminescence from high quality tin oxide nanowires. Appl Phys Lett 95:061908

Cheng CW, Liu B, Yang HY, Zhou WW, Sun L, Chen R, Yu SF, Zhang JX, Gong H, Sun HD, Fan HJ (2009) Hierarchical assembly of ZnO nanostructures on SnO_2 backbone nanowires: low temperature hydrothermal preparation and optical properties. ACS Nano 3:3069

Du N, Zhang H, Yu JX, Wu P, Zhai CX, Xu YF, Wang JZ, Yang DR (2009) Large-scale synthesis of water-soluble nanowires as versatile templates for nanotubes. Chem Mater 21:5264

Feng JJ, Zhu JT, Xu JJ, Chen HY (2009) Enhanced biosensing performance of mesoporous SnO_2 multilayer film in interfacing hemoglobin. J Nanosci Nanotechnol 9:2290

Jia NQ, Xu J, Sun MH, Jiang ZY (2005) A mediatorless hydrogen peroxide biosensor based on horseradish peroxidase immobilized in tin oxide sol-gel film. Anal Lett 38:1237

Kafi AKM, Wu GS, Chen AC (2008) A novel hydrogen peroxide biosensor based on the immobilization of horseradish peroxidase onto Au-modified titanium dioxide nanotube arrays. Biosens Bioelectron 24:566

Liu JP, Li YY, Huang XT, Ding RM, Hu YY, Jiang J, Liao L (2009) Direct Growth of SnO_2 Nanorod array electrode for lithium-ion batteries. J Mater Chem 19:1859

Luongo K, Sine A, Bhansali S (2005) Development of a highly sensitive porous Si-based hydrogen sensor using Pd nano-structures. Sens Actuators B 111–112:125–129

Mishra RL, Mishra SK, Prakash SG (2009) Optical and gas sensing characteristics of tin oxide nano-crystalline thin film. J Ovonic Res 5(4):77–85

Nunes P, Fortunato E, Martins R (2001) Thin film combustible gas sensors based on Zinc. Oxide Mat Res Soc Symp Proc 666

Shen GZ, Chen PC, Ryu K, Zhou CW (2009) Devices and chemical sensing applications of metal oxide nanowires. J Mater Chem 19:828–839

Stanimirova TJ, Atanasov PA, Dimitrov IG, Dikovska AO (2005) Investigation on the structural and optical properties of tin oxide films grown by pulsed laser deposition. J Optoelectron Adv Mater 7(3):1335–1340

Tennakone K, Kumara GRRA, Kottegoda IRM, Perera VPS (1999) An efficient dye-sensitized photoelectrochemical solar cell made from oxides of tin and zinc. Chem Commun (1):15–16. doi:10.1039/A806801A

Zhang Z, Gao J, Wong LM, Tao JG, Liao L, Zheng Z, Xing GZ, Peng HY, Yu T, Shen ZX, Huan CH, Wang SJ, Wu T (2009) Morphology-controlled synthesis and a comparative study of the physical properties of SnO_2 nanostructures: from ultrathin nanowires to ultrawide nanobelts. Nanotechnology 20(13): 135605